Supporting Information for

Nature of Intramolecular Resonance Assisted Hydrogen Bonding in Malonaldehyde and Its Saturated Analogue

Alice Grosch[1], Stephanie C. C. van der Lubbe[1,*], Célia Fonseca Guerra[1,2,*]

[1] Department of Theoretical Chemistry and Amsterdam Center for Multiscale Modeling, Vrije Universiteit Amsterdam, The Netherlands

[2] Leiden Institute of Chemistry, Gorlaeus Laboratories, Leiden University, The Netherlands

S1 Full computational details

All calculations were performed using the Density Functional Theory (DFT) based program Amsterdam Density Functional (ADF) 2016.101.[1,2] We used the Generalized Gradient Approximation (GGA) exchange functional developed by Becke (B),[3] and the GGA correlation functional developed by Perdew (P86).[4] The BP86 functional is in good agreement with the best available ab initio results for the hydrogen bond lengths and energies of DNA base pairs.[5-7] All integrals that are evaluated numerically, including the exchange-correlation integrals, are solved by using the Becke integration scheme with an integration accuracy of 'excellent'.[8]

The Kohn-Sham Molecular Orbitals (KS MOs) are constructed from a linear combination of Slater-type orbitals (STOs), which have the correct cusp behavior and long-range decay. We used the large TZ2P basis set, which is of triple-ζ quality for all atoms and has been augmented with two sets of polarization functions, i.e. $2p$ and $3d$ on H and $3d$ and $4f$ on C, N and O.[9] To speed up the computation, we treated the $1s$ core shells of carbon, nitrogen and oxygen by the frozen-core approximation.[10] The molecular density was fitted by the systematically improvable Zlm fitting scheme with quality 'excellent'.[11] The SCF procedure was considered to be converged if the difference between ρ^n and ρ^{n+1} was equal to or smaller than 1e-6.

Geometries were optimized in the gas phase in delocalized coordinates. The convergence criterion was 1e-5 for the nuclear gradient in Hartree/angstrom. The systems were optimized in C_s symmetry, because the C_s symmetry allows us to decompose the orbital interaction into a σ- and π-contribution (*vide infra*). For 3-OH, the C_s symmetry is not a global minimum structure; the energetic penalty for enforcing a planar geometry is 5.7 kcal mol^{-1}. However, as we are only interested in the nature of the intramolecular hydrogen bond and how it compares with its unsaturated analogue MA, we enforced a planar structure with Cs symmetry for all structures in this work.

1. Te Velde, G.; Bickelhaupt, F. M.; Baerends, E. J.; Fonseca Guerra, C.; van Gisbergen, S. J. A.; Snijders, J. G.; Ziegler, T. Chemistry with ADF. *J. Comput. Chem.* **2001**, *22*, 931-967.

2. Fonseca Guerra, C.; Snijders, J. G.; te Velde, G.; Baerends, E. J. Towards an order-N DFT method. *Theor. Chem. Acc.* **1998**, *99*, 391-403.

3. Becke, A. D. Density-functional exchange-energy approximation with correct asymptotic behavior. *Phys. Rev. A* **1988**, *38*, 3098-3100.

4. Perdew, J. P. Density-Functional Approximation for the Correlation Energy of the Inhomogeneous Electron Gas. *Phys. Rev. B* **1986**, *33*, 8822-8824.

5. Šponer, J.; Jurečka, P.; Hobza, P. Accurate Interaction Energies of Hydrogen-Bonded Nucleic Acid Base Pairs. *J. Am. Chem. Soc.* **2004**, *126*, 10142-10151.

6. Jurečka, P.; Šponer, J.; Černy, J.; Hobza, P. Benchmark Database of Accurate (MP2 and CCSD(T) Complete Basis Set Limit) Interaction Energies of Small Model Complexes, DNA Base Pairs, and Amino Acid Pairs. *Phys. Chem. Chem. Phys.* **2006**, *8*, 1985-1993.

7. Fonseca Guerra, C.; van der Wijst, T.; Poater, J.; Swart, M.; Bickelhaupt, F. M. Adenine versus Guanine Quartets in Aqueous Solution: Dispersion-Corrected DFT study on the Differences in π-stacking and Hydrogen-Bonding Behavior. *Theor. Chem. Acc.* **2010**, *125*, 245-252.

8. Becke, A. D. A Multicenter Numerical Integration Scheme for Polyatomic Molecules. *J. Chem. Phys.* **1988**, *88*, 2547-2553.

9. Snijders, J. G.; Vernooijs, P.; Baerends, E. J. Roothaan-Hartree-Fock-Slater Atomic Wave Functions. Single-Zeta, Double-Zeta, and Extended Slater-Type Basis Sets for $_{87}$Fr-$_{103}$Lr. *At. Data Nucl. Data Tables* **1981**, *26*, 483-509.

10. Baerends, E. J.; Ellis, D. E.; Ros, P. Self-consistent Molecular Hartree-Fock-Slater Calcuations I. The Computational Procedure. *Chem. Phys.* **1973**, *2*, 41-51.

11. Franchini, M.; Philipsen, P. H. T.; van Lenthe, E.; Visscher, L. Accurate Coulomb Potentials for Periodic and Molecular Systems through Density Fitting. *J. Chem. Theory Comput.* **2014**, *10*, 1994-2004.

S2   Bond energy decomposition analysis (EDA) scheme

Additional insight into the hydrogen bonding mechanism is obtained by employing the so-called bond energy decomposition analysis (EDA) scheme.[12] The EDA uses Kohn-Sham molecular orbitals (KS MOs) to decompose the bond energy into several, chemically meaningful terms. Let us start with the (hydrogen) bond energy ΔE, which is defined as:

$$\Delta E = E_{molecule} - E_{fragment1} - E_{fragment2} \tag{1}$$

Here, $E_{molecule}$ is the energy of the fully optimized system with C_s symmetry, and $E_{fragment1}$ and $E_{fragment2}$ are the energies of the fragments optimized in C_1 symmetry, i.e., without any geometrical constraints. The overall bond energy ΔE is made up of two major components:

$$\Delta E = \Delta E_{prep} + \Delta E_{int} \tag{2}$$

In this formula, the preparation energy ΔE_{prep} is the amount of energy required to deform the isolated monomers from their equilibrium structure to the geometry that they have in the interacting system. The interaction energy ΔE_{int} corresponds to the actual energy change when the prepared fragments are combined to form the interacting molecule. The interaction energy can be further decomposed into the electrostatic interaction ΔV_{elstat}, Pauli repulsion ΔE_{Pauli}, orbital interactions ΔE_{oi} and dispersion corrections ΔE_{disp}:

$$\Delta E_{int} = \Delta V_{elstat} + \Delta E_{Pauli} + \Delta E_{oi} \tag{3}$$

The term ΔV_{elstat} is obtained by bringing the fragments from infinity to the positions they have in the interacting system, resulting in an overlap between the unperturbed fragment charge distributions. The accompanied energy change is associated with the electrostatic interaction ΔV_{elstat}, and is usually attractive for neutral systems at equilibrium distance. Next, the wavefunction that is associated with the overlapping charge densities is antisymmetrized (usually by orthogonalization of the fragment orbitals) and renormalized. The resulting energy change is the Pauli repulsion ΔE_{Pauli}, which comprises the destabilizing interactions between occupied orbitals and is responsible for any steric repulsion. Subsequently, the wave function 'relaxes' from the antisymmetrized to the final wave function by mixing in the virtual orbitals into the occupied orbitals. The associated orbital interaction ΔE_{oi} accounts for charge transfer (i.e., donor–acceptor interactions between occupied orbitals on one fragment with unoccupied orbitals on the other fragment, including the HOMO-LUMO interactions) and polarization (empty/occupied orbital mixing on one fragment due to the presence of the other fragment).

The orbital interaction energy can be further decomposed into the contributions from each irreducible representation Γ of the interacting system using the extended transition state (ETS) scheme developed by Ziegler and Rauk:[13-15]

$$\Delta E_{oi} = \Delta E_{\sigma} + \Delta E_{\pi} \tag{4}$$

Our approach differs in this respect from the Morokuma scheme[16,17] which instead attempts a decomposition of the orbital interactions into polarization and charge transfer. In systems with a clear σ/π separation, the symmetry partitioning in our approach proves to be most informative.

The EDA scheme has been successfully applied on resonance-assistance and cooperativity in hydrogen bonds, and accurately reproduces high-level CCSD(T)/CBS benchmark values.[6,18-20] Furthermore, this EDA gives comparable trends to other decomposition schemes such as SAPT.[22,23] For more information on the EDA scheme we refer to the in-depth review by Bickelhaupt and Baerends, 2000.[12]

12.   Bickelhaupt, F. M.; Baerends, E. J. Kohn-Sham Density Functional Theory: Predicting and Understanding Chemistry, in *Reviews in Computational Chemistry*; Lipkowitz, K. B.; Boyd, D. B., Eds.; John Wiley & Sons, Inc., Hoboken, NJ, 2000, Vol. 15, 1-81.

13.   Ziegler, T.; Rauk, A. CO, CS, N_2, PF_3 and $CNCH_3$ as σ Donors and π Acceptors. A Theoretical Study by the Hartree-Fock-Slater Transition-State Method. *Inorg. Chem.* **1979**, *18*, 1755-1759.

14.   Ziegler, T.; Rauk, A. A Theoretical Study of the Ethylene-Metal Bond in Complexes between Cu^+, Ag^+, Au^+, Pt^0, or Pt^{2+} and Ethylene, Based on the Hartree-Fock-Slater Transition-State Method. *Inorg. Chem.* **1979**, *18*, 1558-1565.

15.   Ziegler, T.; Rauk, A. On the Calculation of Bonding Energies by the Hartree Fock Slater method. *Theor. Chi. Acta* **1977**, *46*, 1-10.

16.   Morokuma, K. Molecular Orbital Studies of Hydrogen Bonds. III. C=O•••H-O Hydrogen Bond in H_2CO•••H_2O and H_2CO•••$2H_2O$. *J. Chem. Phys.* **1971**, *55*, 1236-1244.

17.   Kitaura, K.; Morokuma, K. A New Energy Decomposition Scheme for Molecular Interactions Within the Hartree-Fock Approximation. *Int. J. Quantum Chem.* **1976**, *10*, 325-340.

18.   Fonseca Guerra, C.; Bickelhaupt, F. M.; Snijders, J. G.; Baerends, E. J. The Nature of the Hydrogen Bond in DNA Base Pairs: The Role of Charge Transfer and Resonance Assistance. *Chem. Eur. J.* **1999**, *5*, 3581-3594.

19.   Paragi, G.; Fonseca Guerra, C. Cooperativity in the Self-Assembly of the Guanine Nucleobase into Quartet and Ribbon Structures on Surfaces. *Chem. Eur. J.* **2017**, *23*, 3042-3050.

20.   Gao, W.; Feng, H.; Xuan, X.; Chen, L. The Assessment and Application of an Approach to Noncovalent Interactions: the Energy Decomposition Analysis (EDA) in Combination with DFT of Revised Dispersion Correction (DFT-D3) with Slater-Type Orbital (STO) Basis Set. *J. Mol. Model.* **2012**, *18*, 4577-4589.

21.   Hesselmann, A.; Jansen, G.; Schütz. M. Interaction Energy Contributions of H-Bonded and Stacked Structures of the AT and GC DNA Base Pairs from the Combined Density Functional Theory and Intermolecular Perturbation Theory Approach. *J. Am. Chem. Soc.* **2006**, *128*, 11730-11731.

22.   Langlet, J.; Bergès, J.; Reinhardt, P. Decomposition of Intermolecular Interactions: Comparison between SAPT and Density-Functional Decompositions. *J. Mol. Struct.* **2004**, *685*, 43-56.

S3   Contour plots of MA and 3-OH frozen in 3-OH geometry
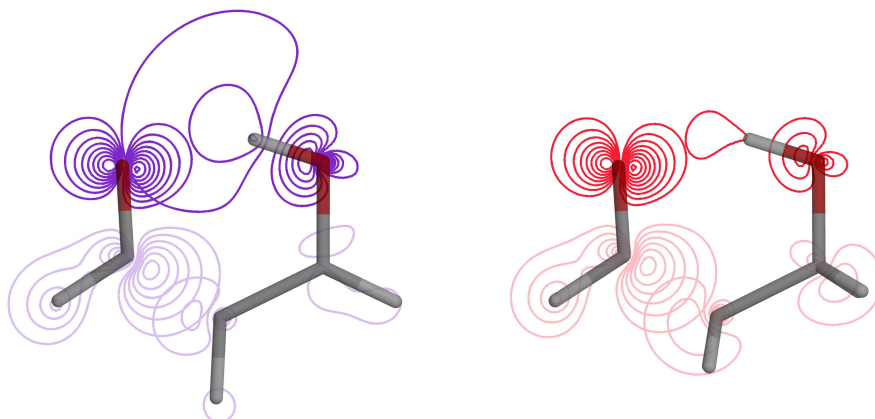
Figure S1. Contour plots [20 contours from 0.09 to 1.0 au (ketone fragment) and from 0.05 to 1.0 au (enol fragment)] of the overlapping HOMO and LUMO orbitals of MA (purple) and 3-OH (red), frozen in 3-OH geometry.

S4 MA, 3-OH, MA$_{minusOH}$ and 3-OH$_{minusOH}$ with and without π virtual orbitals

MA$_{minusOH}$ and 3-OH$_{minusOH}$ are obtained by substituting OH with a hydrogen atom (Figure S2). Only their new hydrogen atom is reoptimized. As can be seen in Table S1, the effect of the π virtual orbitals is identical as in the EE-MA and EE-3-OH structures. This confirms our conclusions that there is no synergistic interplay between the σ and π electron systems.
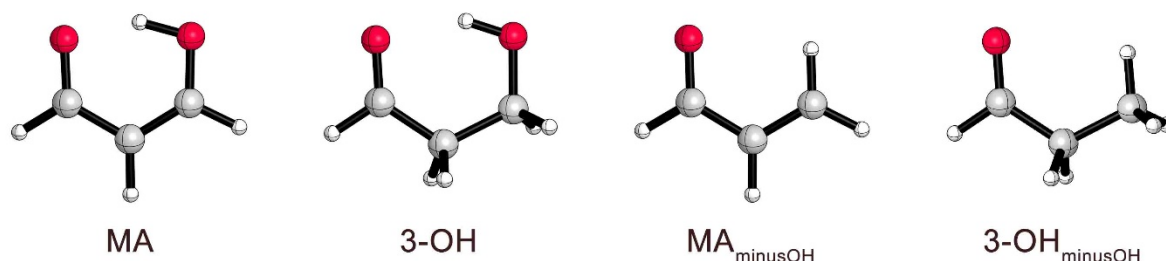
Figure S2. Chemical structures of MA, 3-OH, MA$_{minusOH}$ and 3-OH$_{minusOH}$.

Table S1. Bond energy decomposition analysis [in kcal mol^{-1}] for MA, 3-OH, MA$_{minusOH}$ and 3-OH$_{minusOH}$ with all virtual orbital present [(σ,π)] and with all π virtual orbitals removed [$(\sigma,-)$] at the BP86/TZ2P level of theory.

	ZZ-MA		ZZ-3-OH		MA no OH		3OH no OH	
Virtuals available	(σ,π)	$(\sigma,-)$	(σ,π)	$(\sigma,-)$	(σ,π)	$(\sigma,-)$	(σ,π)	$(\sigma,-)$
ΔE_{int}	-128.9	-93.3	-97.1	-83.8	-105.8	-82.4	-96.2	-83.1
ΔV_{elstat}	-217.6	-217.6	-179.2	-179.2	-203.8	-203.8	-177.7	-177.7
ΔE_{Pauli}	388.3	388.3	318.3	318.3	362.2	362.2	309.9	309.9
ΔE_{σ}	-262.3	-264.0	-221.9	-222.8	-238.5	-240.8	-214.5	-215.3
ΔE_{π}	-37.3	-	-14.3	-	-25.8	-	-13.9	-

S5   Full dataset MA and 3-OH while frozen in each other's equilibrium

Table S2. Bond energy decomposition analysis [in kcal mol^{-1}] for ZZ-MA, ZZ-3-OH, EE-MA and EE-MA with all virtual orbital present [(σ,π)] and with all π virtual orbitals removed [(σ,-)] frozen in MA geometry and 3-OH geometry at the BP86/TZ2P level of theory.

	ZZ-MA		ZZ-3-OH		EE-MA		EE-3-OH	
Virtuals available	(σ,π)	(σ,-)	(σ,π)	(σ,-)	(σ,π)	(σ,-)	(σ,π)	(σ,-)
MA distance (short H-bond)								
ΔE_{int}	-128.9	-93.3	-95.5	-75.7	-116.7	-88.8	-93.4	-77.7
ΔV_{elstat}	-217.6	-217.6	-224.8	-224.8	-197.4	-197.4	-202.1	-202.1
ΔE_{Pauli}	388.3	388.3	418.4	418.4	345.1	345.1	367.9	367.9
ΔE_{σ}	-262.3	-264.0	-267.6	-269.3	-233.7	-236.5	-241.6	-243.5
ΔE_{π}	-37.3	0.0	-21.6	0.0	-30.8	0.0	-17.6	0.0
3-OH distance (long H-bond)								
ΔE_{int}	-123.0	-96.7	-97.1	-83.8	-115.0	-92.0	-93.2	-81.2
ΔV_{elstat}	-171.8	-171.8	-179.2	-179.2	-164.6	-164.6	-170.1	-170.1
ΔE_{Pauli}	293.7	293.7	318.3	318.3	283.4	283.4	304.1	304.1
ΔE_{σ}	-217.2	-218.6	-221.9	-222.8	-209.3	-210.7	-214.3	-215.1
ΔE_{π}	-27.6	0.0	-14.3	0.0	-24.5	0.0	-12.9	0.0

S6 Cartesian coordinates optimized structures

Cartesian coordinates [in Å] and total bonding energies [in kcal mol^{-1}] of all optimized molecules used in this work, computed at BP86/TZ2P.

ZZ–MA (C$_s$)   **[–1247.2]**

C	1.241691	−0.044952	0.000000
O	1.281548	1.212189	0.000000
C	0.018186	−0.781876	0.000000
C	−1.168403	−0.085059	0.000000
O	−1.222414	1.231288	0.000000
H	−0.220992	1.523564	0.000000
H	−2.144819	−0.579047	0.000000
H	2.197421	−0.606171	0.000000
H	0.021486	−1.868889	0.000000

ZZ–3–OH (C$_s$)   **[–1410.7]**

C	1.351515	−0.046473	0.000000
O	1.486075	1.166135	0.000000
C	0.056998	−0.813243	0.000000
C	−1.298309	−0.056987	0.000000
O	−1.226058	1.364488	0.000000
H	−0.278356	1.617173	0.000000
H	2.258922	−0.700665	0.000000
H	0.132298	−1.492859	0.867654
H	0.132298	−1.492859	−0.867654
H	−1.874731	−0.378211	0.884178
H	−1.874731	−0.378211	−0.884178

EE–MA (C$_s$)   **[–1233.0]**

C	−0.681870	−1.255019	0.000000
O	−1.936001	−1.350657	−0.000000
C	0.000000	0.000000	0.000000
C	1.376062	−0.000000	−0.000000
O	2.089214	1.107745	−0.000000
H	1.373684	1.866882	−0.000000
H	1.967885	−0.920411	−0.000000
H	−0.078768	−2.184887	0.000000
H	−0.553292	0.935668	0.000000

EE–3–OH (C$_s$)   **[–1408.6]**

C	0.000000	−0.000000	−0.000000
O	−0.733758	0.974742	−0.000000
C	1.504565	0.000000	0.000000
C	2.285232	−1.341395	0.000000
O	3.705170	−1.243426	0.000000
H	3.940677	−0.291307	0.000000
H	−0.447322	−1.025308	−0.000000
H	1.786133	0.623113	0.867653
H	1.786133	0.623113	−0.867653
H	1.974492	−1.923546	−0.884173
H	1.974492	−1.923546	0.884173

S7   Cartesian coordinates constrained structures

Cartesian coordinates [in Å] and total bonding energies [in kcal mol^{-1}] of molecules with constrained geometry, computed at BP86/TZ2P.

ZZ–MA frozen in 3–OH geometry (C_s) [–1224.0]

C	1.351510	−0.046469	0.000000
O	1.486063	1.166140	0.000000
C	0.056998	−0.813252	0.000000
C	−1.298305	−0.056987	0.000000
O	−1.226048	1.364491	0.000000
H	−0.278346	1.617189	0.000000
H	2.258917	−0.700661	0.000000
H	0.052492	−1.900098	0.000000
H	−2.302145	−0.473364	0.000000

ZZ–3–OH frozen in MA geometry (C_s) [–1387.3]

C	1.241691	−0.044952	0.000000
O	1.281548	1.212189	0.000000
C	0.018186	−0.781876	0.000000
C	−1.168403	−0.085059	0.000000
O	−1.222414	1.231288	0.000000
H	−0.220992	1.523564	0.000000
H	−1.780085	−0.470944	0.859269
H	2.197421	−0.606171	0.000000
H	0.131853	−1.485238	0.853059
H	0.131853	−1.485238	−0.853059
H	−1.780085	−0.470944	−0.859269

EE–MA frozen in 3–OH geometry (C_s) [–1215.4]

C	0.000000	0.000000	0.000000
O	−0.733759	0.974742	0.000000
C	1.504566	0.000000	0.000000
C	2.285233	−1.341395	0.000000
O	3.705170	−1.243427	0.000000
H	3.940677	−0.291307	0.000000
H	−0.447322	−1.025308	0.000000
H	2.076975	0.928970	0.000000
H	1.895611	−2.354593	0.000000

EE–3–OH frozen in MA geometry (C_s) [–1387.5]

C	−0.681871	−1.255019	0.000000
O	−1.936002	−1.350657	0.000000
C	0.000000	0.000000	0.000000
C	1.376062	0.000000	0.000000
O	2.089214	1.107746	0.000000
H	1.373685	1.866882	0.000000
H	1.708319	−0.630128	−0.866483
H	−0.078768	−2.184887	0.000000
H	−0.414844	0.565294	0.865759
H	−0.414844	0.565294	−0.865759
H	1.708319	−0.630128	0.866483